A wind tunnel/HIL setup for integrated tests of Floating Offshore Wind Turbines

IOP Conf. Series: Journal of Physics: Conf. Series **1037** (2018) 052025 doi:10.1088/1742-6596/1037/5/052025

A wind tunnel/HIL setup for integrated tests of Floating Offshore Wind Turbines

I. Bayati[1*], A. Facchinetti[1], A. Fontanella[1], H. Giberti[2] & M. Belloli[1]

1: Politecnico di Milano, Department of Mechanical Engineering, Milano, Italy
2: Universitá degli studi di Pavia, Dipartimento di Ingegneria Industriale e dell'Informazione, Pavia, Italy

E-mail: ilmasandrea.bayati@polimi.it

Abstract. This paper presents the technical issues and methodological aspects concerning hybrid/hardware-in-the-loop (HIL) testing of floating offshore wind turbines (FOWTs) insides the Politecnico di Milano wind tunnel. The scaling issues faced when performing scale model tests on FOWT are presented and the advantages of the HIL methodology with respect to traditional ocean basin tests are shown. The main aspects of the numerical and physical subsystems of the HIL experimental setup are discussed, focussing on their interaction when investigating the effect of aerodynamic loads on the global response of the floating system.

1. Introduction

Floating wind turbines (FOWTs) are well recognized as the key technology to push wind energy further offshore and exploit the high and constant winds of many coastal areas that cannot be reached with traditional offshore solutions [23]. The design of such machines is highly reliant on numerical codes, used to simulate the FOWT response to combined wind and wave loads and provide a deeper understanding of the involved aero-hydrodynamic phenomena. For this approach to be effective, experimental data are needed to calibrate simulation models and to assess their prediction capability with respect to the different operating conditions faced by the wind turbine during its operating life. The high value of full-scale data is usually balanced by the high costs involved in the process of designing and deploying a FOWT prototype and the greater level of uncertainty. By performing tests at model scale it is instead possible to gather data under closely controlled environmental conditions with lower economical and safety risks [1].

Performing scale model experiments on FOWTs is complex since wind and waves loads, gravitational and buoyancy forces, mooring lines and flexible dynamics must be reproduced simultaneously. Ocean basin tests on a complete Froude-scaled model of the floating system were recently performed under different research projects to investigate the dynamics of different FOWT concepts [3]-[9]. From these tests it becomes clear the difficulty of correctly reproducing the wind turbine aerodynamic loads at the low Reynolds number set by Froude scaling [2]. The hybrid/hardware-in-the-loop (HIL) methodology was recently proposed to avoid the above-mentioned problem. According to this technique, the floating wind turbine is split into two complementary subsystems that are demanded to model different physical phenomena. Aerodynamic or hydrodynamic loads are reproduced by means of a physical scale model in

a dedicated facility (respectively wind tunnel or ocean basin) while complementary forces are simulated by the real-time integration of a numerical model of the platform [19]-[21] or the wind turbine rotor [10, 11].

In this work, the peculiarities of the HIL methodology developed at PoliMi in order to perform wind tunnel tests on floating wind turbines are discussed. The Froude-Reynolds conflict is introduced, showing its importance for scale model tests aimed at studying the effect of aerodynamic loads on the overall FOWT response. Then, the hybrid/HIL methodology is explained, discussing the main features of the numerical and physical subsystems. The problematics of wind tunnel HIL testing are introduced and the solutions found by the authors to make the methodology effective are presented.

2. Scaling issues and HIL testing

Scale model tests on FOWTs are especially challenging since it is not possible to achieve satisfactory results by scaling the floating system fixing a unique similitude law. Ocean basin tests are traditionally based on Froude scaling, being Froude number set to be equal for the full-scale system and the scale model

$$Fr = \frac{U^2}{gL} \tag{1}$$

where U is the wind speed, g the gravity constant and L a characteristic length. This scaling approach leads to a unity scale factor for accelerations and allows to correctly model gravity-dependent loads. The common wind tunnel practice instead, tries to approach, at model scale, the full-scale Reynolds number to ensure scaled flow conditions for the system under investigation.

$$Re = \frac{\rho U L}{\mu} \tag{2}$$

where ρ and μ are, respectively, the air density and dynamic viscosity.

The Reynolds number scale factor λ_{Re} for different combinations of length scale factor λ_L and velocity scale factor λ_v is by surface of Figure 1 (the scale factor for the generic quantity X is the ratio between a given quantity evaluated at prototype and model scale, $\lambda_x = X_p/X_m$). All values of λ_{Re} are greater than one, meaning that any considered combination of λ_L and λ_v results in a scale-model Reynolds number lower than target. When Froude number similitude is required, being the gravity constant g fixed for the model and full-scale systems, the velocity scale λ_v directly depends on the length scale λ_L according to Equation 3, represented in Figure 1 by the red line.

$$\lambda_v = \sqrt{\lambda_L} \tag{3}$$

If Reynolds similitude is required, the air properties equal for the model and full-scale systems, the velocity scale is function of λ_L only, as shown by Equation 4, that corresponds to the yellow line of Figure 1.

$$\lambda_v = 1/\lambda_L \tag{4}$$

The incompatibility between Froude and Reynolds scaling is evident and this conflict sets a major constraint for experiments where the model of the complete floating wind turbine has to be used (i.e. traditional ocean basin tests). If Froude scaling is used, length scale factors between 50 and 100, required to fit a multi-megawatt wind turbine in a common testing facility, lead to a velocity scale factor between 7 and 10 and a Reynolds number that is between 350 and 1000 times lower than the one experienced by the full-scale system. This sets a hard constraint for the scaling of the wind turbine rotor [18] and for the correct reproduction of aerodynamic loads in traditional ocean basin tests.

The HIL methodology was proposed as a potential solution to the Froude-Reynolds conflict, making possible to correctly reproduce the FOWT aerodynamics and hydrodynamics in scale

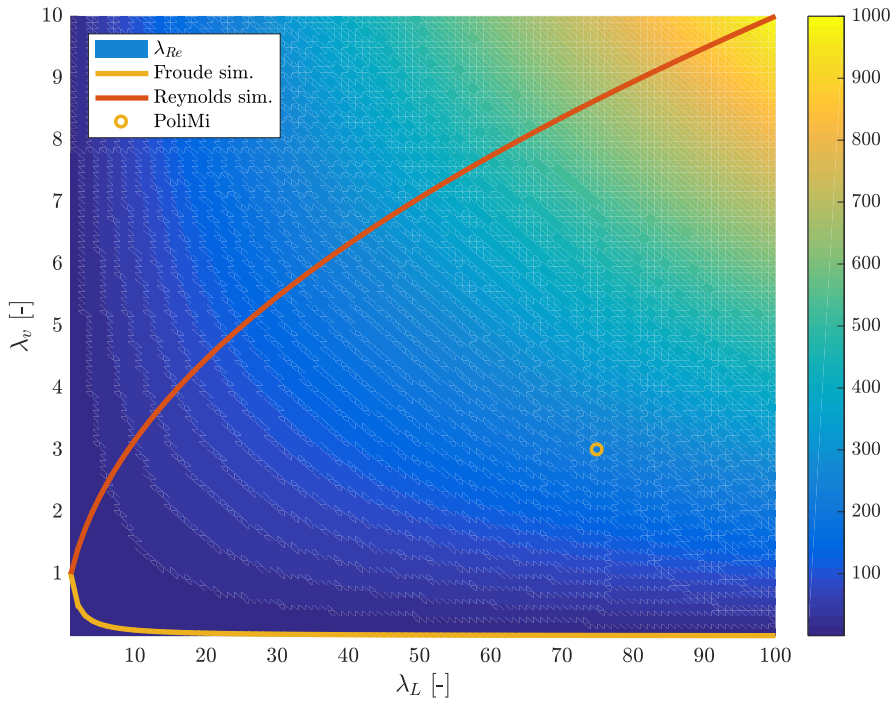

Figure 1. Reynolds number reduction factor for different scaling procedures.

model experiments. An increasing interest has been recently put in the study of the interaction between unsteady aerodynamics, the turbine controller action and the platform dynamics [7, 8]. The hybrid/HIL methodology developed at PoliMi makes possible to investigate these topics directly inside a wind tunnel, exploiting the high quality flow conditions offered by the test facility. The HIL system currently used for tests is presented in detail in [19]-[21] whereas an in-deep discussion of experimental results for a 2-DOFs system can be found in [22]. The floating wind turbine, is divided into two complementary subsystems: the first one, that models the wind turbine aerodynamic loads, is reproduced by a physical scale model of the wind turbine (WTM), placed inside the atmospheric boundary layer (ABL) test section of the Politecnico di Milano (PoliMi) wind tunnel (GVPM, [12]). The other subsystem, that is implemented numerically, models the floating structure dynamics, the hydrodynamic loads due to incident waves and mooring lines response. The floating structure rigid-body resulting from real-time integration of the floating system numerical model are fed to a 6-DOFs robot that moves consistently the wind turbine scale model.

The adoption of the HIL methodology relaxed the scaling constraints for the wind tunnel experiments, and allowed to independently set the length and velocity scale factors [14] In particular, λ_L was fixed to 75 to limit the wind tunnel blockage effect avoiding, at the same time, an excessive miniaturization of the model components. The velocity scale factor λ_v was instead set to 3 to limit the Reynolds number reduction and have reasonable design requirements for the model actuators and for the natural frequencies of aeroelastic components. The other scale factors for HIL experiments were derived from dimensional analysis and are reported in Table 1. As shown in Figure 1 the combination of λ_L and λ_v chosen for the PoliMi experiments (yellow ◯) leads to a much lower Reynolds number reduction than what would have been achieved with Froude scaling for the same model size.

Table 1. Scale factors for the PoliMi WTM.

Scale	Expression	Value
Length	λ_L	75
Velocity	λ_v	3
Mass	$\lambda_M = \lambda_L^3$	75^3
Time	$\lambda_T = \lambda_L/\lambda_v$	25
Frequency	$\lambda_\omega = \lambda_v/\lambda_L$	$1/25$
Acceleration	$\lambda_a = \lambda_v^2/\lambda_L$	$3^2/75$
Force	$\lambda_f = \lambda_L^2\lambda_v^2$	$75^2 \cdot 3^2$

3. The hybrid/HIL methodology

The HIL methodology for wind tunnel tests on FOWT is resumed in Figure 2. The FOWT

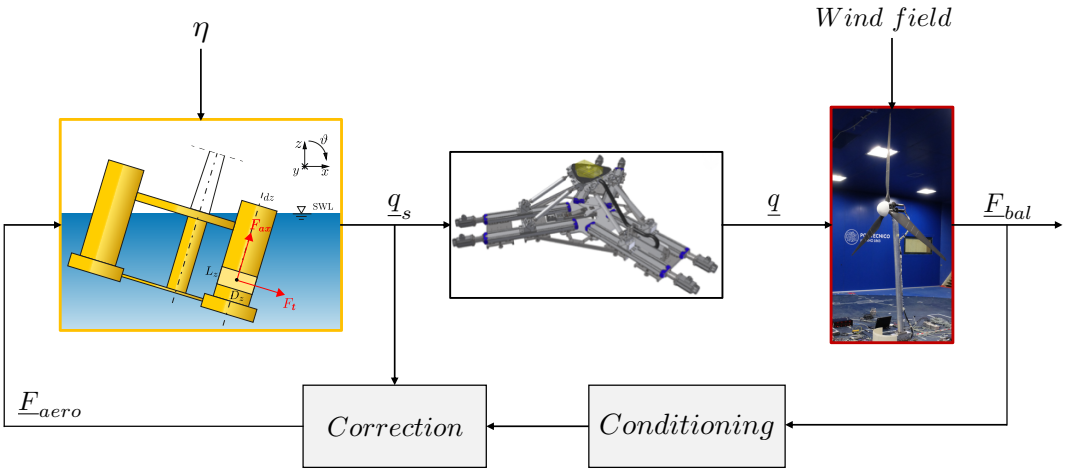

Figure 2. Scheme of the HIL methodology.

response to wind and wave loads is governed by Equation 5 that is used for real-time integration and is represented by the leftmost block of Figure 2.

$$[M]_f\ \underline{\ddot{q}}_s + [K]_f\ \underline{q}_s = (\underline{F}_{hst} + \underline{F}_{moor} + \underline{F}_{hydro}) + \underline{F}_{aero} \tag{5}$$

The absolute platform translations and tilt rotations (respectively surge, sway, heave, roll, pitch, yaw) collected by vector $\underline{\ddot{q}}_s = [x, y, z, \rho, \theta, \sigma]^T$ are the set-points for the 6-DOFs robot controller.

On the left-hand side of Equation 5 are collected the FOWT inertial and gravitational loads which reproduction is entirely demanded to the numerical subsystems. The non-unity acceleration scale factor (see Table 1) makes impossible to reproduce the wind turbine gravitational restoring with the scale model. To scale the wind turbine mass is an hardly achievable goal, since this is in large part set by commercial components [14, 15]. To avoid the consequent uncertainties in the simulation of the FOWT response, it was preferred to model also inertial loads relying on the numerical subsystem [19].

On the right-hand side of Equation 5 are instead collected aerodynamic and hydrodynamic loads on the FOWT structure. The hydrostatic restoring forces on the platform $\underline{F}_{hst}$, the

gravitational loads $\underline{F}_{grav}$, the hydrodynamic loads $\underline{F}_{hydro}$ are computed from the platform hydrodynamic model as function of the simulated platform state $\underline{q}_s$ and the height of incoming waves η. A dedicated numerical model allows to simulate the dynamic response of mooring lines and to define the restoring forces $\underline{F}_{moor}$. Aerodynamic loads $\underline{F}_{aero}$ are introduced in the experimental set-up by the rotor of the wind turbine scale model.

The above mentioned sub-structuring offers a significative advantage. The physical setup is optimized to reproduce the aerodynamic loads of a specific wind turbine concept, whereas the correct modeling of structural and hydrodynamic loads is demanded to the numerical subsystem. Once the aerodynamic performance of the wind turbine scale model rotor is known and uncertainties of the HIL methodology itself are defined, it is possible to test different FOWT concepts with the same setup. Differently from ocean basin tests (either conventional or hybrid) it is not required to design and build a platform model for each FOWT concept to be tested, avoiding the introduction of unknown measurement uncertainties [25].

Implementing the HIL methodology is however a difficult task. Significative computational resources are needed to run the model of the floating structure and to process in real-time the signal acquired from the physical subsystem. Imperfections in the measurement of the aerodynamic loads may lead to uncertainties in the floating platform dynamic response. In [22] results from a preliminary hybrid/HIL test campaign on a 2-DOFs model (surge and pitch) of the DeepCwind floating system are presented and analyzed in order to identify any possible source of error introduced by the HIL methodology.

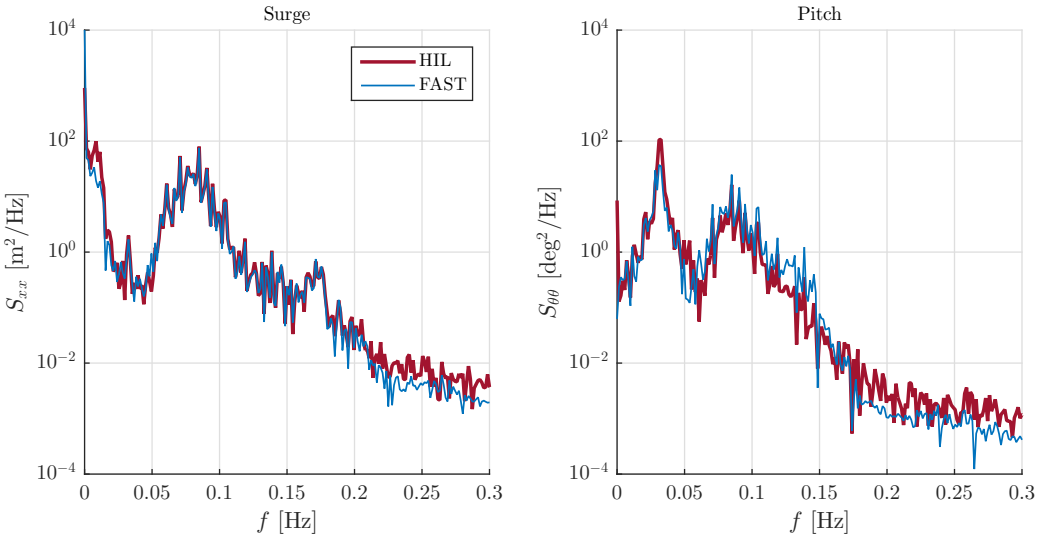

Figure 3. PSD of the measured surge and pitch response for Operational waves and no wind.

An example is shown In Figure 3, where the PSD of the platform DOFs response for Operational waves (full-scale significative height H_s 7.10 m and peak period T_p 12.10 s) is compared to the outputs of equivalent numerical simulations performed in the aero-servo-hydro-elastic simulation code FAST. The overall matching between FAST simulation and the experimentally measured platform response is good across the frequency range of interest and especially in the linear wave excitation range. Some minor differences can be seen in the low-frequency range (platform rigid-body motion modes natural frequencies) and, for the pitch DOF only, for frequencies above 0.15 Hz. The major source of uncertainty were identified in the response of the hydraulic actuation system that was used in placed of the 6-DOFs robot.

4. Aerodynamic loads

Aerodynamic loads are reproduced by the rotor of the physical wind turbine scale model in the ABL tests section of the PoliMi wind tunnel. FOWT dynamics can be investigated in laminar flow (longitudinal turbulence index I_u 1.5%) as well as under specific atmospheric boundary layer wind conditions, reproduced by means of turbulence generators and roughness elements placed in the test chamber upwind the model. Generic environmental conditions consisting of combined stochastic wind and waves are simulated generating irregular waves from an assigned power-spectral density and controlling the wind profile and turbulence levels.

Force measurements $\underline{F}_{bal}$ from the 6-components load cell mounted at the wind turbine tower base are processed to extract the aerodynamic loads $\underline{F}_{aero}$, that are fed-back to the real-time model. In the assumption of a rigid wind turbine, the forces measured by the load cell are expected to follow Equation 6.

$$\underline{F}_{bal} = \underline{F}_{aero} + [M]_t \ddot{\underline{q}} + [K]_t \underline{q} \tag{6}$$

where $[M]_t$ and $[K]_t$ are respectively the wind turbine inertia tensor and gravitational stiffness matrix with respect to rigid-body platform DOFs, and $\underline{q}$ is the vector of the actual displacements and rotations of the wind turbine scale model. The aerodynamic loads are then obtained subtracting from the load cell signals a so-called correction force $\underline{F}_{corr}$.

$$\underline{F}_{corr} = [M]_t^* \ddot{\underline{q}}_s + [K]_t^* \underline{q}_s \tag{7}$$

where $\underline{q}_s$ is the vector of the wind turbine displacements and rotations resulting from the real-time model integration (i.e. differences between $\underline{q}_s$ and $\underline{q}$ are introduced by the 6-DOFs robot and the relative control system). $[M]_t$ and $[K]_t$ are the inertia tensor and gravitational stiffness matrix of the wind turbine model. The structural properties required to define the above mentioned matrices are estimated from experimental tests, as explained in [20] for a 2-DOFs configuration.

In Figure 4 the PSD of the surge and pitch components of $\underline{F}_{bal} = [F_x, M_y]^T$, $\underline{F}_{corr}$ and the difference ($\underline{F}_{res}$) are shown for Operational waves (full-scale significative height Hs 7.10 m and peak period Tp 12.10 s) and no wind conditions. The correction forces estimated as

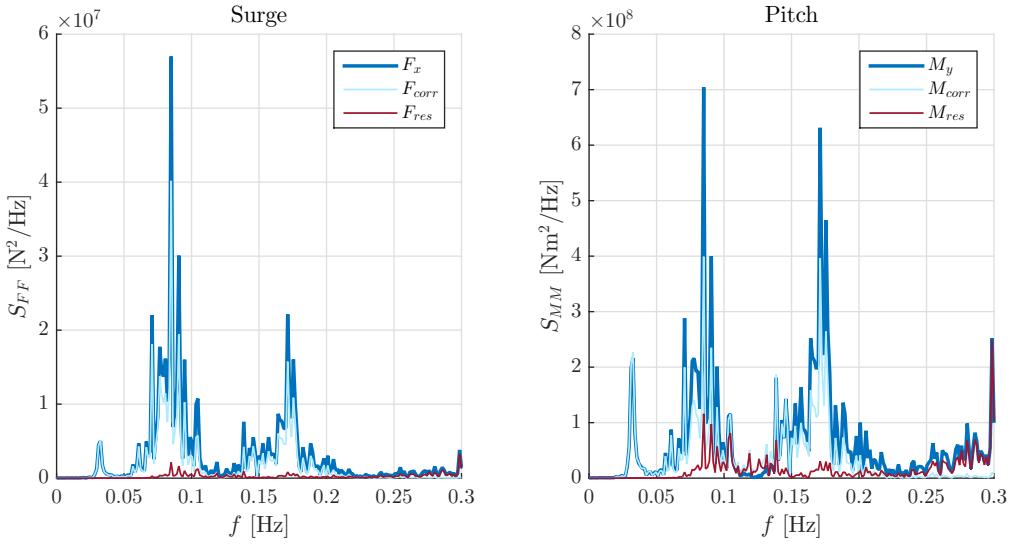

Figure 4. PSD of the surge and pitch forces for for Operational waves and no wind.

in Equation 7 are very close to the measured forces and give an almost null residual force in the low-frequency range, where it is more important to investigate the effect of aerodynamic loads. Some differences are present in the high-frequency range, especially for the pitch DOF, and the magnitude of the residual force is not negligible only here. Errors in the estimation of the wind turbine model structural properties and actuation delays (that are responsible of the difference between $\underline{q}_s$ and $\underline{q}$) are the main cause of residual forces. The effect of flexibility of the WTM components is not considered in Equation 7 and introduces some deviations of $\underline{F}_{corr}$ from $\underline{F}_{bal}$ especially at higher frequencies, where it becomes more evident. Low-pass filtering of the platform displacements $\underline{q}_s$ computed from the real-time model proved to be an effective solution for semi-submersible platforms.

5. Floating platform model

The numerical subsystem is demanded to model the hydrodynamic loads while respecting the hard real-time constraints required by the HIL methodology. For this reason it was not possible to use standard codes for the design of FOWTs but a ad-hoc model was specifically developed for the application [21].

The buoyancy restoring is introduced in the model in a linearized form, reported in Equation 8.

$$\underline{F}_{hst} = -[K]_{grav} \cdot \underline{q}_s \tag{8}$$

where $[K]_{hst}$ is the hydrostatic stiffness matrix, resulting from 3D panel codes pre-simulation runs.

Mooring dynamics is generally affected by evident nonlinearities and linear force-displacement relationships are unsuitable to describe the recall forces by the anchoring system. In HIL experiments, a lumped-mass model of the mooring lines is integrated, together with the floating structure model, to reproduce the mooring system dynamics. The model is based on an optimized number of nodes, lower that those generally used by the most common simulation codes, making possible to simulate with the mooring line response with a good fidelity but low computational efforts.

Hydrodynamic loads $\underline{F}_{hydro}$ of Equation 5 accounts for the forces resulting from the integration of the dynamic pressure of water over the floating platform surface. These loads, expressed by Equation 9, are the combination of radiation forces, viscous forces and loads from incident-wave scattering (diffraction) forces.

$$\underline{F}_{hydro} = \underline{F}_{rad} + \underline{F}_{visc} + \underline{F}_{diff} \tag{9}$$

The calculation of radiation forces $\underline{F}_{rad}$ requires the solution of a convolution integral between the platform velocities $\underline{q}_s$ and the retardation matrix $[K(t)]$ (impulse response), that describes the energy dissipation due to the wave radiation from when the platform is oscillating in still water [26]. Computing the radiation convolution integral is a time consuming task. The memory effect was then modeled exploiting the state space approximation of [27], as shown in [19]. Also the calculation of diffraction forces proved to be challenging when performed under the strict real-time requirements of HIL testing [21]. The first and second order diffraction forces $\underline{F}_{diff}$ are computed at each integration step from the wave spectrum and the complex, frequency dependent transfer functions resulting from panel code pre-simulation. This was preferable instead of relying on pre-computed, multidimensional lookup tables of hydrodynamic forces time histories.

6. Wind turbine scale model

The physical subsystem is the wind turbine scale model (WTM) placed in the GVPM ABL test section. The model currently used for HIL experiments is based on the properties of the DTU

10MW concept [13], currently used as reference wind turbine for different international research projects. The general model configuration and a detail of the rotor-nacelle assembly (RNA) are shown in Figure 5.

Figure 5. General view of the wind turbine scale model (left) and detail of the rotor-nacelle assembly (right).

The wind turbine rotor is the result of a performance scaling procedure [16], where blades were re-designed to match the full-scale wind turbine aerodynamic performance and aeroelastic response in the scaled environment faced in the wind tunnel. An aero-elastic optimization procedure, described in detail in [16], was used to achieve the reference thrust coefficient, considered of major importance for FOWTs dynamics, the isolated blade first flap-wise natural frequency and the overall rotor weight. The experimental WTM rotor performance in terms of power coefficient C_P and thrust coefficient C_T, measured for different combinations of tip-speed ratio λ and rotor collective pitch angle β, are shown in Figure 6. The general shape of the

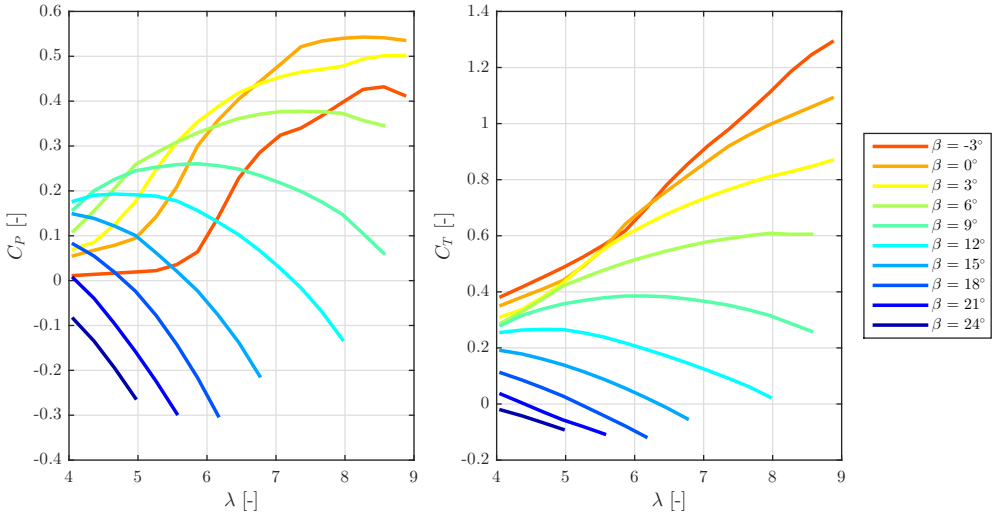

Figure 6. Power and thrust coefficients for the PoliMi WTM for different values of tip-speed-ratio λ and pitch angle β.

coefficients curves and punctual values for $\lambda = 5-8$ are close to those of the DTU 10MW RWT.

A complex mechatronic system is mounted on-board the PoliMi WTM [13, 14]. An electronically commuted (EC) motor and a dedicated servo-controller are used to regulate the rotor torque. The full-span pitch angle of each blade is independently controlled by a dedicated servo-motor housed on-board the hub. An embedded control system based on *NI Veristand* provides the interface with actuators and measurement instruments on-board the scale model. The WTM aerodynamic performance and the mechatronic setup make possible to implement on the model full-scale control logic without significative modifications. The interaction between the floating structure dynamics, wind and wave loads and controller action can be directly investigated.

7. The HexaFloat robot

The physical and numerical subsystems are effectively joined together by a 6-DOFs parallel kinematic machine (PKM). The HexaFloat, shown in Figure 7,was designed to move the wind turbine scale model according to the computations of the floating system numerical model [17]. The parallel kinematic configurations was chosen for the high stiffness, low sensitivity of the end-

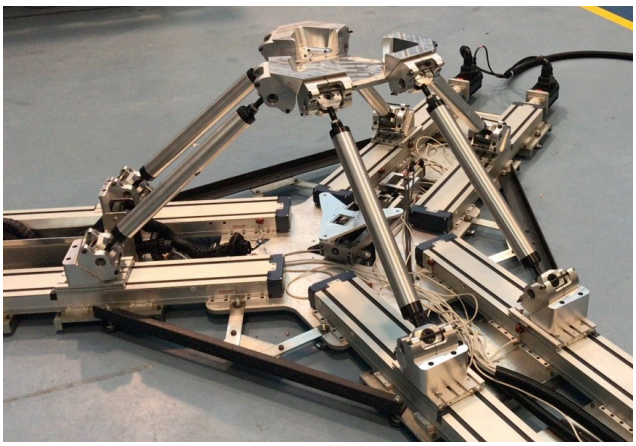

Figure 7. The 6-DOFs HexaFloat robot.

effector position to the different error sources, and the low height of the tool center point (TCP). This, in particular, was needed to have the rotor of the wind turbine model at a reasonable distance from the wind tunnel ceiling. A genetic algorithm was used to optimize the 6-DOFs robot layout [28] to ensure the workspace required by hybrid/HIL experimental tests and respect the kinematic, kineostatic and geometric constraints of the PKM.

8. Conclusions

This paper describes an innovative testing technique to study integrated dynamics of floating wind turbines inside an atmospheric boundary layer wind tunnel. Hybrid/HIL testing allows to solve the Froude-Reynolds conflict that penalizes the correct reproduction of the wind turbine aerodynamics in traditional ocean basing scale model tests. By relying on a physical model only for the reproduction of aerodynamic loads generated by the wind turbine rotor it is possible to focus experiments on the investigation of the interaction between floating platform rigid-body motion modes, unsteady aerodynamics and wind turbine controller action. By simulating the platform dynamics and the hydrodynamic forcefield it is possible to avoid measurement uncertainties related to design and realization of a platform scale model. The authors' efforts for the characterization of the error sources introduced by the HIL methodology are summarized and the main solutions found to reduce their effect on the experiments are shown.

References

[1] Bottasso C. L.. Campagnolo F. and Petrovic V. (2014) *Wind tunnel testing of scaled wind turbine models: Beyond aerodynamics*. Journal of Wind Engineering and Industrial Aerodynamics.
[2] Martin H. R., Kimball R. W., Viselli A. M. et al. (2012) *Methodology for Wind/Wave Basin Testing of Floating Offshore Wind Turbines*. Proceedings of the ASME 31st International Conference on Ocean, Offshore and Arctic Engineering, OMAE.
[3] Goupee A. J., Koo B. J., Kimball R. W. et al. (2014) *Experimental Comparison of Three Floating Wind Turbine Concepts*. Journal of Offshore Mechanics and Arctic Engineering. DOI: 10.1115/1.4025804.
[4] Koo B. J., Goupee A. J., Kimball R. W. et al. (2014) *Model Tests for a Floating Wind Turbine on Three Different Floaters*. Journal of Offshore Mechanics and Arctic Engineering. DOI: 10.1115/1.4024711.
[5] Stewart G., Lackner M., Robertson A. et al. (2012) *Calibration and Validation of a FAST Floating Wind Turbine Model of the DeepCwind Scaled Tension-Leg Platform*. Conference Paper, National Renewable Energy Laboratory.
[6] Anant J., Robertson A. N., Jonkman J. M. et al. (2012) *FAST Code Verification of Scaling Laws for DeepCwind Floating Wind System Tests*. Conference Paper, National Renewable Energy Laboratory.
[7] Yu W., Lemmer F., Bredmose H. et al. (2017) *The TripleSpar Campaign: Implementation and Test of a Blade Pitch Controller on a Scaled Floating Wind Turbine Model*. 14th Deep Sea Offshore Wind R&D Conference EERA DeepWind.
[8] Goupee A. J., Kimball R. W., Dagher H.J. (2017) *Experimental observations of active blade pitch and generator control influence on floating wind turbine response*. Renewable Energy.
[9] Robertson A. N., Wendt F., Jonkman J. M. et al. (2017) *OC5 Project Phase II: Validation of Global Loads of the DeepCwind Floating Semisubmersible Wind Turbine*. 14th Deep Sea Offshore Wind R&D Conference EERA DeepWind.
[10] Sauder T., Chabaud V., Thys M. et al. (2016) *Real-Time Hybrid Model Testing of a Braceless Semi-submersible Wind Turbine. Part I: the Hybrid Approach*. International Conference on Offshore Mechanics and Arctic Engineering - OMAE.
[11] Bachynski E. E., Thys M., Sauder T. et al. (2016) *Real-Time Hybrid Model Testing of a Braceless Semi-submersible Wind Turbine. Part II: Experimental Results*. International Conference on Offshore Mechanics and Arctic Engineering - OMAE.
[12] GVPM wind tunnel. http://www.windtunnel.polimi.it
[13] Bak C. et al. (2013) *Description of the DTU 10MW Reference Wind Turbine*. DTU Wind Energy Report.
[14] Bayati I., Belloli M., Bernini L. et al. (2017) *Scale model technology for floating offshore wind turbines*. IET Renewable Power Generation. DOI: 10.1049/iet-rpg.2016.0956 IET Digital Library
[15] Bayati I., Bernini L., Fiore E. et al. (2016) *On the functional design of the DTU 10MW wind turbine scale model of LIFES50+ project*. Journal of Physics Conference Series 735(5). DOI: 10.1088/1742-6596/753/5/052018
[16] Bayati I., Bernini L., Belloli M. et al. (2017) *Aerodynamic design methodology for wind tunnel tests of wind turbine rotors*. Journal of Wind Engineering and Industrial Aerodynamics. DOI: 10.1016/j.jweia.2017.05.004
[17] Bayati I., Belloli M., Ferrari D. et al.(2014) *Design of a 6-DoF Robotic Platform for Wind Tunnel Tests of Floating Wind Turbines*. Energy Procedia, Volume 53, pp. 313-323. DOI: 10.1016/j.egypro.2014.07.240
[18] De Ridder R. J., Otto W., Zondervan G. J. et al. (2014) *Development of a Scaled-Down Floating Wind Turbine for Offshore Basin Testing*. Proceedings of the 33th international Conference on Ocean, Offshore and Arctic Engineering, OMAE.
[19] Bayati I., Belloli M. and Facchinetti A. (2017) *Wind tunnel 2-DOF Hybrid/HIL tests on the OC5 floating offshore wind turbine*. Proceedings of the 36th international Conference on Ocean, Offshore and Arctic Engineering, OMAE. DOI: 10.1115/OMAE2017-61763
[20] Ambrosini S., Bayati I., Facchinetti A. et al. (2018) *Methodological and technical aspects of a 2DoF/HIL setup for wind tunnel tests of floating systems*. **Forthcoming**.
[21] Bayati I., Facchinetti A., Fontanella A. et al. (2018) *6-DOF Hydrodinamic Modelling for Wind Tunnel Hybrid/HIL Tests of FOWT: the Real-Time Challenge*. Proceedings of the 37th international Conference on Ocean, Offshore and Arctic Engineering. **Forthcoming**.
[22] Bayati I., Facchinetti A., Fontanella A. et al. (2018) *Analysis of FOWT dynamics in hybrid 2-DOF HIL wind tunnel experiments*. Ocean Engineering. **Forthcoming**.
[23] EU H2020 LIFES50+. http://http://lifes50plus.eu
[24] Matha D., Schlipf M., Cordle A. et al. (2011). *Challenges in Simulation of Aerodynamics, Hydrodynamics, and Mooring-Line Dynamics of Floating Offshore Wind Turbines*. Proceedings of the International Offshore and Polar Engineering Conference.
[25] Robertson A. (2017). *Uncertainty Analysis of OC5-DeepCwind Floating Semisubmersible Offshore Wind Test*

Campaign. Proceedings of the International Offshore and Polar Engineering Conference.
[26] Faltinsen O. M. (1990). *Sea Loads on Ships and Offshore Structures*. Cambridge University Press, Cambridge, UK.
[27] Perez T., Fossen T. I. (2009). *A matlab toolbox for parametric identification of radiation-force models of ships and offshore structures*. Modeling, Identification and Control, 30(1), pp. 1?15.
[28] Fiore E., Giberti H. (2016). *Optimization and comparison between two 6-DoF parallel kinematic machines for HIL simulations in wind tunnel*. MATEC Web of Conferences.